

## Methylene Blue sorption by the chemically modified *Ocimum basilicum* leaves powder

Suhair A. Bani-Atta<sup>a</sup>, Hatem A. Al-Aoh<sup>a,\*</sup>, Meshari M.H. Aljohani<sup>a</sup>, Ali A. Keshk<sup>a</sup>, Hamza S. Al-Shehri<sup>b</sup>, Syed Khalid Mustafa<sup>a</sup>, Nasser A. Alamrani<sup>a</sup>, Ahemed A.A. Darwish<sup>c,d</sup>, Mohamed Sobhi<sup>a</sup>

<sup>a</sup>Department of Chemistry, Faculty of Science, University of Tabuk, Tabuk 71491, Saudi Arabia, Tel. +6-537692007; emails: issa\_hatem2@yahoo.com/halawah@ut.edu.sa (H.A. Al-Aoh), Tel. +6-535817359; emails: s\_bantatta@yahoo.com/s\_bantatta@ut.edu.sa (S.A. Bani-Atta), Tel. +6-553063991; email: mualjohani@ut.edu.sa (M.M.H. Aljohani), Tel. +6-535830353; email: akeshk@ut.edu.sa (A.A. Keshk), Tel. +6-531210675; email: syed.pes@gmail.com (S.K. Mustafa), Tel. +6-556552576; email: nalomrani@ut.edu.sa (N.A. Alamrani), Tel. +6-535846573; email: mohamedsob7i@yahoo.com (M. Sobhi)

<sup>b</sup>King Khaled Military Academy, SANG, Jeddah, Saudi Arabia, Tel. +6-506376383; email: h.s.alshehri@outlook.com

<sup>c</sup>Department of Physics, Faculty of Education at Al-Mahweet, Sana'a University, Al-Mahweet, Yemen, Tel. +6-535846573; email: aaadarwish@gmail.com

<sup>d</sup>Department of Physics and Nanotechnology Research Unit, Faculty of Science, University of Tabuk, Tabuk 71491, Saudi Arabia

Received 20 August 2020; Accepted 24 January 2021

---

### ABSTRACT

Chemically modified *Ocimum basilicum* leaves powder (CMOBLP) adsorbent was used for the elimination of Methylene Blue (MB) from aqueous solutions. The morphology of CMOBLP was identified by microscopy of scanning electron and Fourier transform infrared technics. The porosity and surface area of the prepared CMOBLP have also been determined by applying a Brunauer–Emmett–Teller (BET) surface analyzer. The influences of MB primary concentration, temperature, sorption time, and solution pH were studied. The parameters of kinetics were evaluated, and the obtained results suggest that MB sorption by CMOBLP follows the model of the second-order. Thermodynamic outcomes pointed to that the MB sorption by CMOBLP is exothermic and spontaneous. Isotherm models of Langmuir, Freundlich, and Temkin were applied, and the experimental data were fitted well with the model of Langmuir, proposing monolayer sorption. The present study strongly reveals that CMOBLP is a very effective adsorbent. The sorption capacities of 714.29, 666.67, 625.00, and 555.56 mg/g were obtained at 20°C, 30°C, 40°C, and 50°C, respectively.

**Keywords:** Sorption; Methylene Blue; *Ocimum basilicum* leaves powder; Isotherm; Kinetic; Thermodynamic

---

### 1. Introduction

Methylene blue (MB) as a cationic dye has been widely used for multiple purposes, especially wood and silk dyeing, hair coloring, rubber, and food industries [1–6], wastewaters generated from the above-mentioned industries contain non-negligible amounts of MB [7]. Due to the

constant structure of MB, and its inability for biodegradation, the usage of this dye will cause various noticeable environmental problems [8,9]. Moreover, MB is considered very toxic and has very negative effects, whether for humans, animals, marine life, or plants [10,11]. For these reasons, the industrial wastewaters contaminated by MB must be treated before their discharge. Various chemical and physical methods were applied for the treatment of

---

\* Corresponding author.

contaminated waters from MB and other hazardous pollutants [12,13]. Among these methods, sorption is an effective method that has been widely used as a straightforward and low-cost process [13]. In addition to the higher efficiency of the sorption technique, its usage is not accompanied by the formation of any secondary pollution during the treatment process [14,15].

The oldest adsorbent used in this technique is activated carbon in its three shapes (granular, powder, and fiber) [16,17]. For example, activated carbon was used for the sorption of methylene blue [18], Congo red [19], malachite green dye [20], and other contaminants from aqueous solutions. Despite the high sorption rate and higher efficiency of activated carbon towards organic and inorganic pollutants, the high cost of this adsorbent is the biggest obstacle to its usage in treating contaminated waters.

Recently, several attempts have been carried out to use nanoparticles (NP<sub>s</sub>) in the field of treating the polluted waters from dyes like MB, heavy metals, and phenols. For example, metal oxides NP<sub>s</sub> such as TiO<sub>2</sub>, Fe<sub>2</sub>O<sub>3</sub>, CuO, and others have been applied for MB sorption from wastewater [21–26]. Unfortunately, with the higher cost of NP<sub>s</sub> preparation, the difficulty of their application in water treatment, and its less sorption efficiency, this type of adsorbent becomes practically undesirable.

For these reasons, attention has turned to prepare adsorbents with low-cost and acceptable effectiveness, additionally to the possibility of preparation and reasonable application in the treatment of polluted waters. Therefore, researchers developed effective adsorbents from low-cost materials to sorption some dyes like MB from industrial wastewaters. For instance, sugar beet pulp [27], mango leaf powder [28], seed shells [29], cashew nutshell [30], spent mushroom substrate [31], natural clay [32], corn cob powder calcined [33], neem leaves powder [34], residue walnut shell [35], and others have been used as new and very cheap adsorbents for MB elimination from wastewater samples.

Ocimum is an aromatic plant that grows in Asia and African regions, common in the Arab world by Habag or Reyhan. It is a non-toxic substance and widely used as a flavoring substance for tea and food due to its distinctive smell. Traditionally Ocimum leaves have been used as medicine for colic ulcer and skin infection treatment [36]. Ocimum seeds are used as bio-sorbents for heavy metals [37–39]. Recently, it is used as a natural coagulant for Congo red removal from wastewater [40]. Till now, there are no work has been carried out to investigate the usage of this plant as a natural adsorbent for MB sorption. Therefore, the current study aimed to synthesize a new adsorbent from *Ocimum basilicum* leaves powder to be used as an effective eliminating agent for MB from wastewater.

The influences of temperature, pH, shaking time, MB initial concentration will be studied in this work. Thermodynamics, kinetics, and isotherms parameters of this sorption will also be estimated.

## 2. Methodology

### 2.1. CMOBLP preparation and characterization

The dried leaves of *Ocimum* plants were bought from the spice shop. In the beginning, the leaves have been

separated from the other parts of plants and powdered by using mortar. The produced powder was cleaned with distilled water various times, then, it was boiled with distilled water for 30 min, after that the leaves powder was separated from the mixture. A 250 mL of 30% w/w of ZnCl<sub>2</sub> solution was mixed with the leaves powder and refluxed for 2 h. The solid powder was separated from the mixture by filtration using a Buchner funnel. The solid part was boiled with 2 M HCl solution for 20 min, following by filtration and washing many times with distilled water till getting a clear filtrate. The adsorbent powder was dried for 13 h in an oven at 120°C. In the end, it was grinding again and sifted with a sieve (diminutions). The resulting powder was kept in a desiccator to be used in the treatment processes.

The pH<sub>ZPC</sub> of the adsorbent was assigned according to Theydan and Ahmed [41] method. The Fourier-transform infrared (FT-IR; Nicolet iS5 of Thermo Scientific FT-IR, US) technique was utilized to specify the functional groups on the surface of CMOBLP. The adsorbent porosity and adsorbent surface area have also been identified from the Brunauer–Emmett–Teller (BET) isotherm of the surface analyzer (NOVA-2200 Ver. 6.11). Scanning electron microscopy (SEM) instrument was applied to specify the CMOBLP surface morphology.

### 2.2. Influence of adsorbent dosage

The sorption process consisted of contacting 15 mL of MB dye solution with a concentration of 500 mg/L with 0.005, 0.010, 0.015, 0.020, 0.025, 0.030, and 0.035 g CMOBLP was carried out at 30°C, initial pH solution, and 170 rpm for 26 h. after that, MB solutions were separated from CMOBLP by filtration and the remaining concentrations of MB in the filtrates were measured by 6800 UV-visible spectrophotometers (Jenway 6800, UK) at λ<sub>max</sub> of 617 nm. Finally, Eq. (1) was applied for the calculation of percentage removal (%R).

$$\% R = \frac{(C_i - C_e)}{C_i} \times 100 \quad (1)$$

where  $C_i$  and  $C_e$  are MB concentrations before and after sorption, respectively.

### 2.3. Effect of solution pH

To study the influence of solution pH on this sorption, six solutions of MB with a fixed concentration (500 mg/L) and different pH values (2–12) were prepared using 1 M of NaOH and HCl solutions. A 15 mL of each solution was mixed with 0.015 g CMOBLP in a 25 mL amber bottle. These six bottles were then put in a shaker incubator for 26 h at 30°C and speed of 170 rpm, followed by filtration for each sample. After sorption, MB concentrations were measured at λ<sub>max</sub> = 617 nm, by means of a UV-visible spectrophotometer (Jenway 6800). Finally, the sorption quantity at equilibrium was evaluated by applying Eq. (2):

$$q_e = \frac{V}{m} (C_i - C_e) \quad (2)$$

where  $q_e$  (mg/g) is the sorption capacity at equilibrium,  $C_i$  is the initial dye concentration,  $C_e$  is the MB concentrations at equilibrium,  $V$  (L) is the volume of adsorbate solution, and  $m$  (g) is the amount of adsorbent.

#### 2.4. Equilibrium and thermodynamic studies

To investigate the influence of initial concentration, temperature, and to determine the parameters related to the isotherm and thermodynamic of this sorption, ten MB solutions with initial concentrations of 200; 300; 400; 500; 600; 700; 800; 1,000; 1,200; and 1,400 mg/L were prepared from the stock solution (5,000 mg/L). A 15 mL was taken from each solution and added to 0.015 g of synthesized adsorbent in a 25 mL amber bottle; the shaking process was carried out for each mixture for 26 h at 20°C and speed of 170 rpm, followed by filtration. The UV-visible measurements were performed to measure the final concentration in the filtrate. Eq. (1) was applied to calculate the amount of MB adsorbed.

The previously mentioned procedures were also conducted at 30°C, 40°C, and 50°C to determine thermodynamic parameters and to investigate the influence of temperature on MB sorption by this adsorbent. Eqs. (3)–(6) have been used to evaluate each of Langmuir, Freundlich, and Temkin isotherm parameters, respectively:

$$\frac{C_e}{q_e} = \frac{1}{q_{\max} K_L} + \frac{C_e}{q_{\max}} \quad (3)$$

$$R_L = \frac{1}{1 + K_L C_i} \quad (4)$$

$$\ln(q_e) = \ln(K_f) + \frac{1}{n} \ln(C_e) \quad (5)$$

$$q_e = B_1 \ln(K_T) + B_1 \ln(C_e) \quad (6)$$

where  $q_{\max}$  (mg/g) represents the maximum capacity of this sorption,  $K_L$ ,  $K_f$ , and  $K_T$  are constants of Langmuir, Freundlich, and Temkin models, correspondingly.  $R_L$  and  $C_i$  are the Langmuir dimensionless factor and the adsorbate highest concentration, respectively.  $n$  is the intensity of the sorption constant, and  $B_1$  is a constant associated with the heat of sorption.

Thermodynamic parameters ( $\Delta H^\circ$ ,  $\Delta S^\circ$ ,  $\Delta G^\circ$ ) of the sorption process were evaluated by applying Eqs. (7) and (8). Since  $\Delta H^\circ$ ,  $\Delta S^\circ$ , and  $\Delta G^\circ$  are the enthalpy, entropy, and free energy changes at the standard conditions, correspondingly:

$$\ln K_C = \frac{\Delta H^\circ}{RT} + \frac{\Delta S^\circ}{R} \quad (7)$$

$$\Delta G^\circ = \Delta H^\circ - T\Delta S^\circ \quad (8)$$

where  $R$  and  $T$  are the general gas constant (0.008314 kJ/K mol) and sorption temperature (Kelvin), respectively.

#### 2.5. Kinetic studies

15 mL of 200, 300, and 400 mg/L of MB solutions have been shaken with 0.015 g of the prepared adsorbent at a rotation speed of 170 rpm and 30°C for 5 min. Each mixture was filtered, and the final concentrations of MB in the filtrate have been measured using a UV/visible spectrometer. Eq. (9) was applied for computing the sorption quantities for each time  $t$  (min).

$$q_t = \frac{V}{m}(C_i - C_t) \quad (9)$$

where  $q_t$  is the sorption capacity at time  $t$ ,  $C_i$  represents the initial dye concentration, and  $C_t$  represents dye concentrations at time  $t$ .  $V$  and  $m$  are the solution volume and adsorbent mass.

The same procedures at the same conditions were repeated for various period times ranged from 10 to 960 min to investigate the effect of adsorption time and to identify the parameters of kinetics.

The linear expressions for the first-order [Eq. (10)], second-order [Eq. (11)], and intra-particle distribution [Eq. (12)] were employed for computing the values of kinetic parameters.

$$\log(q_e - q_t) = \log(q_e) - K_1 \frac{t}{2.303} \quad (10)$$

$$\frac{t}{q_t} = \frac{1}{K_2 (q_e)^2} + \frac{t}{q_e} \quad (11)$$

$$q_t = K_{\text{dif}} \sqrt{t} + C \quad (12)$$

whereas  $q_e$  refers to sorption capacity at equilibrium and  $q_t$  is the sorption capacity after each time interval ( $t$ ).  $C$  is a kinetic parameter associated with the boundary-layer width. The terms  $K_1$ ,  $K_2$ , and  $K_{\text{dif}}$  are the rate constants of the first-order, second-order, and intra-particle distribution kinetic models, in that order.

### 3. Results and discussion

#### 3.1. CMOBLP properties

The microstructure of CMOBLP (SEM spectrum) before sorption is shown in Fig. 1. This spectrum demonstrates that there are multiple and different macropores and gaps on the CMOBLP surface. These holes and macropores have a positive and significant effect on the process of sorption. Because the cations of MB diffuse across the micropores easily to the sorbent effective sites through these gups and macropores.

To determine the  $\text{pH}_{\text{ZPC}}$  for this adsorbent,  $\text{pH}_i$  values were plotted against  $\text{pH}_f - \text{pH}_i$  (Fig. 2). From this Fig. 2, 8.3 was found to be the  $\text{pH}_{\text{ZPC}}$  of this sorbent. Since the CMOBLP surface charge will be negative and positive when the solution pH is higher and less than 8.3.

The FT-IR spectrum (image not presented) showed five main absorption bands (1,516.21; 1,629.33; 1,047.00;

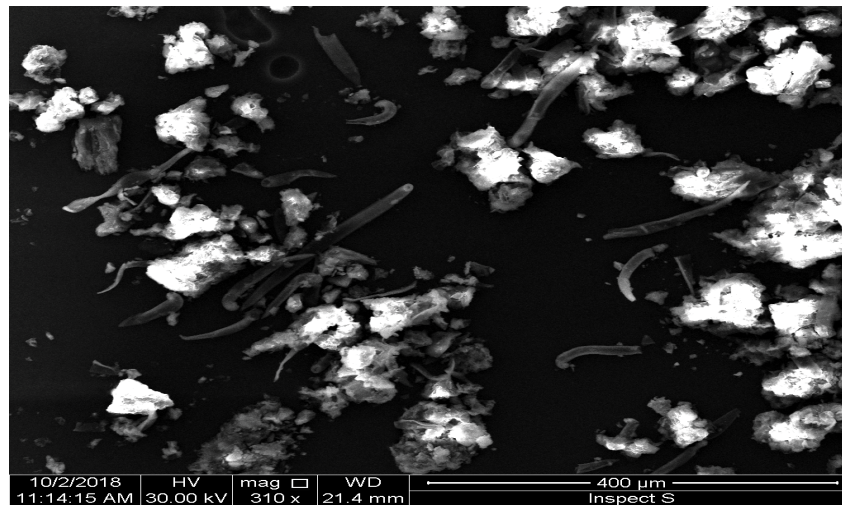


Fig. 1. SEM spectrum of CMOBLP.

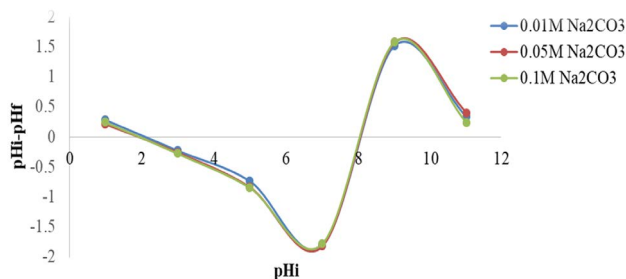


Fig. 2. pH<sub>ZPC</sub> of CMOBLP.

2,929.88; and 3,294.93  $\text{cm}^{-1}$ ). 1,516.21 and 1,629.33  $\text{cm}^{-1}$  bands are assigned to stretching vibration of the ring and  $-\text{NH}_2$  deformation, respectively. Whereas the bands of 1,047.00; 2,929.88; and 3,294.93  $\text{cm}^{-1}$  are related to stretching of C–O, CH, and  $-\text{NH}$ , correspondingly. The sorption process is affected by the sorbent functional groups.

The total pore volume for all pores of a diameter smaller than 2,570.951 Å, average pore diameter, and the area of the adsorbent surface are 0.00711  $\text{cc/g}$ , 264.144 Å, and 117.27  $\text{m}^2 \text{g}^{-1}$ , respectively.

### 3.2. Adsorbent dosage influence

It was found in this work that the values of %R were increased from 40.3% to 76.4% and almost be constant when the mass of CMOBL was increased from 0.005 to 0.015 g and 0.015 to 0.035 g, respectively. Therefore, 0.015 g of this adsorbent was selected in this research as the optimal dosage and used for performing the other experiments.

### 3.3. Effect of pH solution

The results related to solution pH influence on the sorption of MB by CMOBLP are demonstrated in Fig. 3. This figure indicates that the efficiency of sorption is slightly and abruptly increased by increasing pH values in the ranges of 2–8 and 8–12, respectively.

MB as a cationic dye positively charges ions when dissolved in water, and the CMOBLP surface will be positively charged at low pH values. Therefore, the electrostatic repulsion forces will be high at a low pH. Then the number of positive charges on the adsorbent surface is gradually and slightly decreased by increasing pH in the range of 2–8. Thus, the repulsion forces are gradually decreased. This represents the real reason for the slight increase in the efficiency of sorption when pH increased from 2 to 8. While at the pH value over 8, the adsorbent surface charge begins to shift to a positive charge. Thus, the attraction forces will be created between cations of MB and the negative surface charge of CMOBLP, resulting in a sharp increase in the amount of MB adsorbed by CMOBLP. Similar behavior has been observed for other synthesized adsorbents [33,35,42].

### 3.4. Equilibrium and thermodynamic studies

#### 3.4.1. Concentration and temperature influences

The results related to the influence of MB initial concentration and temperature on this sorption performance are illustrated in Fig. 4. Fig. 4 specifies that the amount of sorption increases by increasing MB concentration from 200 to 1,000  $\text{mg/L}$  because the increment of adsorbate concentration overcomes the resistance of the mass transfer between the aqueous medium and solid. Whereas the amount of sorption is constant over 1,000  $\text{mg/L}$  because there is no empty sorption active site to adsorb other MB cations after this concentration. Previous studies showed the same results for MB sorption by different adsorbents [30].

On the contrary, rising temperature decreases the sorption efficiency (Fig. 4). Since the bonding strength between the active adsorbent sites and adsorbate cations decreases with increasing temperature, as well as the solubility of MB is increased by elevated temperature. These outcomes prove that this sorption is an exothermic process in which the direction of equilibrium will be shifted from sorption to desorption (Le Chatelier's principle) [26]. Fig. 4 confirmed that the highest  $q_e$  obtained

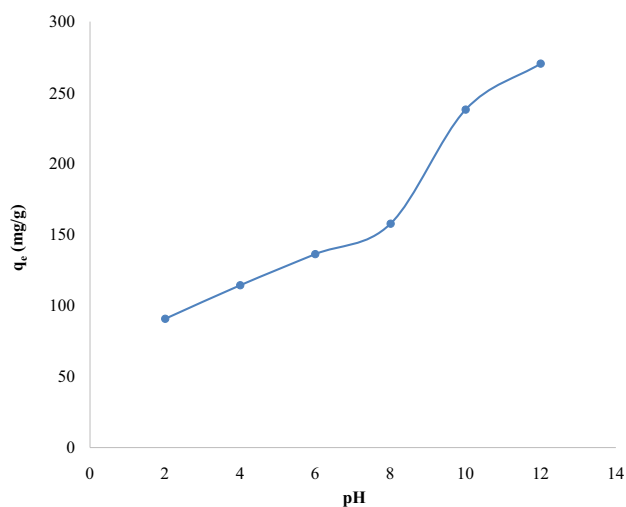


Fig. 3. Effect of pH solution on MB sorption by CMOBLP.

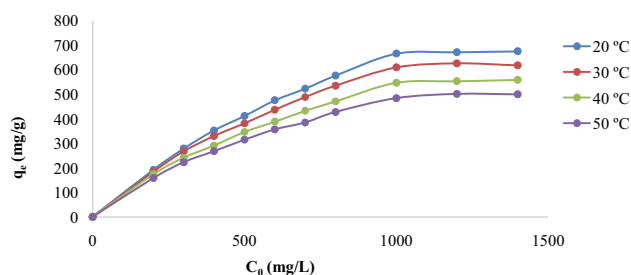


Fig. 4. Influences of temperature and MB initial concentration on the sorption performance of CMOBLP.

was 675.92 at 1,000 mg/L and 20°C. These outcomes are consistent with the previous study [42].

### 3.4.2. Isotherm studies

The interaction between MB cations and CMOBLP surface and the relationship between MB sorption capacity and its concentration at equilibrium has been described by the leaner form of Langmuir, Freundlich, and Temkin isotherm models.  $C_e/q_e$  vs.  $C_e$  (Langmuir model),  $\ln q_e$  vs.  $\ln C_e$  (Freundlich model), and  $q_e$  vs.  $\ln C_e$  (Temkin model) were plotted as represented graphically in Fig. 5. The parameters of MB sorption by the surface of CMOBLP were computed from the intercepts and slopes of these plots and recorded in Table 1. According to  $R^2$  values (Table 1), the highest values were obtained in the Langmuir model, which designates that the experimental data of this sorption were described well by the Langmuir isotherm model. These results prove monolayer sorption of MB dye over homogeneous adsorbent active sites; therefore, a saturation point of MB sorption is reached at equilibrium, and no other MB adsorption can occur after this point. These results are fully compatible with the results obtained for MB adsorption by activated carbon [43]. According to Langmuir model results (Table 1), the highest value of MB amount adsorbed by CMOBLP ( $q_{\max}$ ) is 714.29 mg/g at 20°C. The value of  $R_L$

can also be used to estimate if a certain isotherm is favorable ( $0 < R_L < 1$ ) or not ( $R_L > 1$ ). In Langmuir isotherm, the  $R_L$  values were in the range of 0.02–0.06, and this confirms that the MB sorption by CMOBLP is favorable ( $0 < R_L < 1$ ).

### 3.4.3. Thermodynamic studies

The calculated values of  $\ln K_c$  were plotted as  $1/T$  for sorption of 200, 300, 400, 500, 600, and 700 mg/L MB solution by CMOBLP (figure not presented). Intercepts and slopes of these plots have been used for the calculation of  $\Delta S^\circ$  and  $\Delta H^\circ$  values. In contrast,  $\Delta G^\circ$  values were calculated by applied Eq. (7). Thermodynamic parameter values are recorded in Table 2.

According to the negative values of  $\Delta H^\circ$  (Table 2), MB sorption by CMOBLP is an exothermic process. These results agree well with the results observed in the case of concentration and temperature effects (section 3.4.1), which proved that the capacity of sorption was the highest at low temperatures. The calculated values of  $\Delta H^\circ$  ranged from  $-23.5403$  to  $-49.5373$ , which means the chemisorption process.

The negative  $\Delta S^\circ$  values are decreased with increasing the MB concentration, indicating that the random degree is reduced during the process of sorption. Table 2 also demonstrates that the values of  $\Delta G^\circ$  are negative and reduced by increasing temperature. This verifies that this sorption is a spontaneous process, and the degree of spontaneously is reduced by rising temperature. These results are similar to the result observed in the case of MB sorption by montmorillonite [42], and *Ficus carica* bast-based activated carbon [43].

## 3.5. Kinetic studies

### 3.5.1. Contact time effect

The experimental values of  $q_t$  (sorption capacity at time  $t$ ) were plotted against  $t$  (sorption contact time) to examine the effect of agitation time on the sorption of 200, 300, and 400 mg/L of MB solution by CMOBLP (Fig. 6). Based on Fig. 7, the sorption capacity is elevated by increasing the time of contact from 5 to 180 min, then becomes steady above 180 min for each concentration. It can also be observed from Fig. 6 that the sorption capacity ( $q_t$ ) increased by increasing the MB initial concentration. This indicates an agreement between the result obtained in this part and part related to the effect of adsorbate initial concentration (section 3.4.1 concentration and temperature influences).

### 3.5.2. Kinetic parameters

To specify the MB sorption mechanism by this adsorbent, the experimental sorption data for three concentrations were examined by applying for the first-order [Eqs. (9) and (10)] second-order, and [Eq. (11)] diffusion of intra-particle kinetic models.

The  $\log(q_e - q_t)$  vs.  $t$  (first-order),  $t/q_t$  vs.  $t$  (second-order), and  $q_t$  vs.  $t^{1/2}$  (intra-particle-diffusion) were graphically plotted and illustrated in Figs. 7a–c, respectively. The parameters of kinetics were evaluated from these plots and reported along with the related values of  $R^2$  in Table 3.

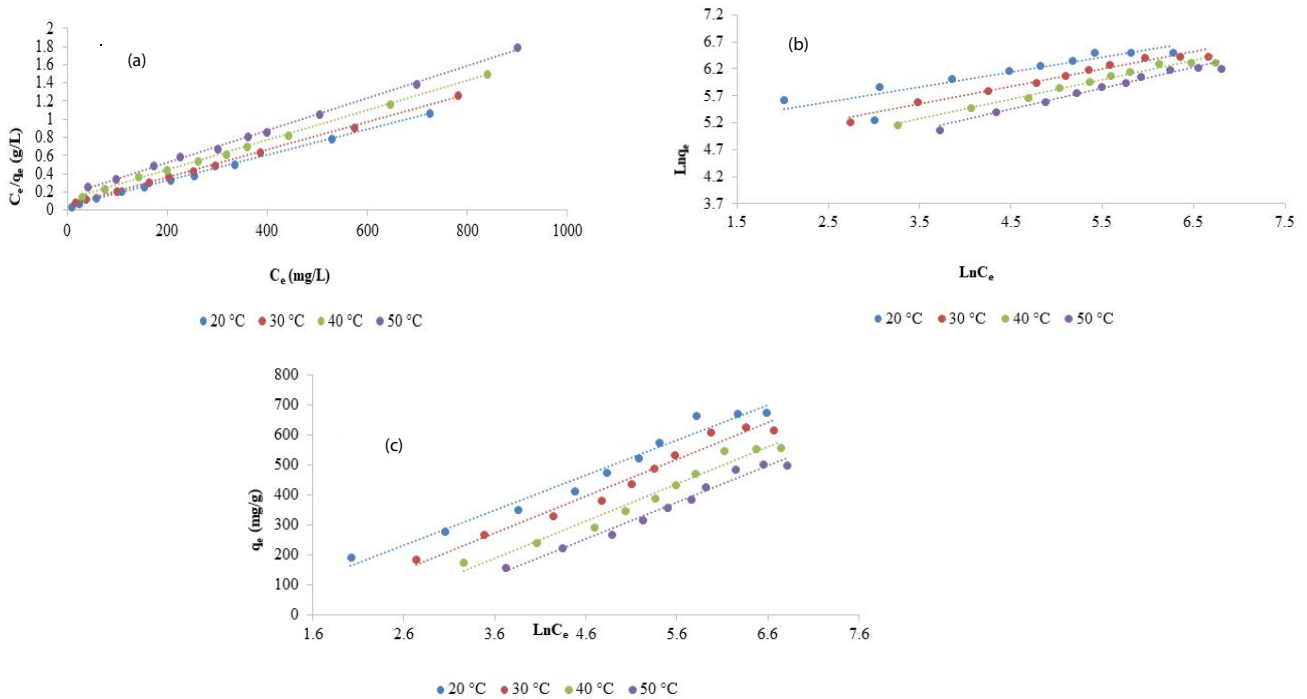


Fig. 5. Langmuir (a), Freundlich (b), and Temkin (c) isotherm for MB sorption by CMOBLP.

Table 1  
Isotherm parameters for MB sorption by CMOBLP

Temperature	Isotherm model											
	Langmuir				Freundlich					Temkin		
	$q_{max}$ (mg/g)	$K_L$ (L/mg)	$R_L$	$R^2$	$K_F$ (mg/g) (L/mg) <sup>1/n</sup>	1/n	n	$R^2$	$K_T$ (L/mg)	$B_1$	$R^2$	
20°C	714.29	0.033	0.021	0.999	134.72	0.275	3.638	0.814	0.531	117.36	0.971	
30°C	666.67	0.026	0.027	0.999	84.167	0.320	3.126	0.972	0.256	122.51	0.971	
40°C	625.00	0.014	0.048	0.999	56.486	0.358	2.797	0.979	0.126	124.04	0.967	
50°C	555.56	0.010	0.064	0.999	40.764	0.387	2.582	0.974	0.080	122.33	0.980	

Table 2  
Thermodynamic parameters for MB sorption by CMOBLP

Initial concentration (mg/L)	$\Delta H^\circ$ (kJ/mol)	$\Delta S^\circ$ (kJ/mol)	$\Delta G^\circ$ (kJ/mol)				$R^2$
			293 K	303 K	313 K	323 K	
200	-49.5373	-0.142	-7.82077	-6.39700	-4.97323	-3.54945	0.998
300	-40.8550	-0.118	-6.31980	-5.14112	-3.96244	-2.78377	0.989
400	-35.3445	-0.104	-4.89689	-3.85772	-2.81855	-1.77939	0.988
500	-26.6198	-0.078	-3.74254	-2.96175	-2.18095	-1.40016	0.999
600	-25.5057	-0.076	-3.23795	-2.47796	-1.71797	-0.95798	0.993
700	-23.5403	-0.071	-2.71317	-2.00235	-1.29153	-0.58071	0.993

The highest  $R^2$  values (Table 3) were found in the case of second-order. Moreover, the sorption capacity calculated at equilibrium ( $q_{e,cal}$ ) by applying the second-order model are almost equal to the amounts of sorption, which are

experimentally determined ( $q_{e,exp}$ ). These outcomes are evidence that the MB sorption by CMOBLP is chemisorption. The results obtained in this section are fully compatible with the thermodynamic results.



Table 3  
Parameters of the first-order and second-order kinetic models for MB sorption by CMOBLP

$C_0$ (mg/L)	$q_{e,exp}$ (mg/g)	$q_{e,cal}$ (mg/g)	Kinetic model					
			First-order			Second-order		
			$K_1$ (h <sup>-1</sup> )	$R^2$	$q_{e,cal}$ (mg/g)	$K_2$ (g/mg h)	$R^2$	Rate
200	185.60	41.57	0.0044	0.936	185.19	0.00050	0.999	0.092308
300	250.89	65.18	0.0037	0.907	250.00	0.00028	0.999	0.070796
400	284.23	69.39	0.0051	0.966	285.71	0.00032	0.999	0.091864

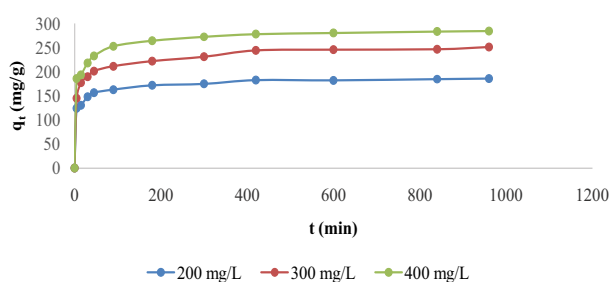


Fig. 6. Relationship between the sorption capacities and contact time for MB sorption by CMOBLP.

It is clear from Fig. 7c that there are two sorption regions in the intra-particle diffusion model. Furthermore, the values of  $R^2$  (Table 4) are small for both regions. This is an indicator that confirms that the intra-particle diffusion does not contribute to the rate of this sorption. MB sorption by coconut husk fiber-based activated carbon gave similar results for this work [18].

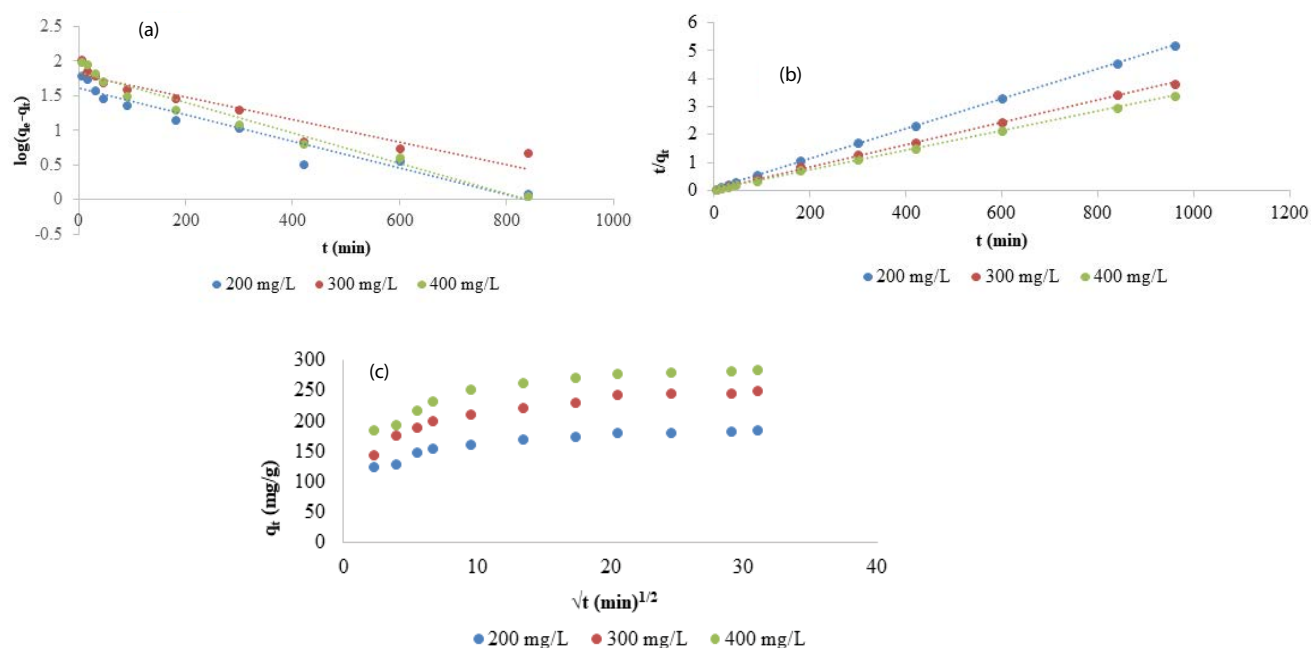


Fig. 7. First-order (a), second-order (b), and diffusion of intra-particle (c) kinetic models for MB sorption by CMOBLP.

### 3.6. Comparison study

The sorption capacities of CMOBLP used in this work and the other low-cost adsorbents previously used towards MB are displayed in Table 5. Following outputs from this table, CMOBLP prepared and applied in this study has the highest sorption capacity toward MB. This invites those interested in treating water to use CMOBLP in the elimination of MB from wastewater.

## 4. Conclusions

This work displayed that CMOBLP has sufficient sorption capacity towards MB. The kinetic, thermodynamic, isotherm parameters, and factors affecting the sorption have been examined. The outcomes obtained confirmed that the MB initial concentration and solution pH have positive effects on the sorption, but this sorption is negatively affected by rising temperature. The experimental data were analyzed by the isotherm models of Langmuir, Freundlich, and Temkin. It was found that the model of Langmuir is the best. The parameters of kinetics are strongly confirmed that

Table 4  
Parameters of the intra-particle diffusion model for MB sorption by CMOBLP

$C_0$ (mg/L)	Region I			Region II		
	$K_{dif}$ (mg/h <sup>1/2</sup> g)	C	$R^2$	$K_{dif}$ (mg/h <sup>1/2</sup> g)	C	$R^2$
200	5.7626	112.26	0.922	0.777	162.48	0.872
300	8.7283	136.16	0.888	1.5161	205.5	0.853
400	9.8635	161.61	0.975	1.072	252.67	0.918

Table 5  
Sorption capacities of CMOBLP and other low-cost adsorbents toward MB

Adsorbents	$q_{max}$ (mg/g)		Sources
CMOBLP	714.29	20°C	Present study
CMOBLP	666.67	30°C	Present study
CMOBLP	625.00	40°C	Present study
CMOBLP	555.56	50°C	Present study
NiO nanoparticles absorbent	166.67		[26]
CuO nanoparticles absorbent	50.25		[26]
Sugar beet pulp	250.01		[27]
Mango leaf powder	156		[28]
Cashew nut shells	476		[30]
Spent mushroom substrate	63.5		[31]
Corn cob powder	46.28		[33]
Orange peel-modified phosphoric acid	307.63		[44]
Neem ( <i>Azadirachta indica</i> ) leaves	60.60		[45]
Teak tree bark	333		[46]
Sunflower seed husk	45.25		[47]
Hazelnut shell	76.9		[48]

the sorption of MB by CMOBLP follows the second-order kinetic model. The Thermodynamic results indicated that MB sorption by CMOBLP is an exothermic and spontaneous process. The highest sorption capacity of CMOBLP toward MB makes it a better choice than other adsorbents. This invites to pay attention and highlights more to use CMOBLP to deduce MB dye from aqueous media.

### Acknowledgments

The authors are very thankful to the Faculty of Science at the University of Tabuk for their support and facilities to finish this work.

### References

- [1] A.M. Vargas, A.L. Cazetta, M.H. Kunita, T.L. Silva, V.C. Almeida, Adsorption of methylene blue on activated carbon produced from flamboyant pods (*Delonix regia*): study of adsorption isotherms and kinetic models, *Chem. Eng. J.*, 168 (2011) 722–730.
- [2] A. Özer, G. Dursun, Removal of methylene blue from aqueous solution by dehydrated wheat bran carbon, *J. Hazard. Mater.*, 146 (2007) 262–269.
- [3] L.W. Low, T.T. Teng, A.F. Alkarkhi, A. Ahmad, N. Morad, Optimization of the adsorption conditions for the decolorization and COD reduction of methylene blue aqueous solution using low-cost adsorbent, *Water Air Soil Pollut.*, 214 (2011) 185–195.
- [4] A.B. Albadarin, C. Mangwandi, Mechanisms of Alizarin Red S and Methylene blue biosorption onto olive stone by-product: isotherm study in single and binary systems, *J. Environ. Manage.*, 164 (2015) 86–93.
- [5] D. Mitrogiannis, G. Markou, A. Çelekli, H. Bozkurt, Biosorption of methylene blue onto *Arthrospira platensis* biomass: kinetic, equilibrium and thermodynamic studies, *J. Environ. Chem. Eng.*, 3 (2015) 670–680.
- [6] M.A. Mohammed, A. Shitu, A. Ibrahim, Removal of Methylene Blue using low-cost adsorbent: a review, *Res. J. Chem. Sci.*, 4 (2014) 91–102.
- [7] J. Beltrán-Heredia, J. Sánchez-Martín, M.A. Dávila-Acedo, Optimization of the synthesis of a new coagulant from a tannin extract, *J. Hazard. Mater.*, 186 (2011) 1704–1712.
- [8] H. Hayat, Q. Mahmood, A. Pervez, Z.A. Bhatti, S.A. Baig, Comparative decolorization of dyes in textile wastewater using biological and chemical treatment, *Sep. Purif. Technol.*, 154 (2015) 149–153.
- [9] K.B. Tan, M. Vakili, B.A. Horri, P.E. Poh, A.Z. Abdullah, B. Salamatinia, Adsorption of dyes by nanomaterials: recent developments and adsorption mechanisms, *Sep. Purif. Technol.*, 150 (2015) 229–242.
- [10] M.T. Yagub, T.K. Sen, S. Afroz, H.M. Ang, Dye and its removal from aqueous solution by adsorption: a review, *Adv. Colloid Interface Sci.*, 209 (2014) 172–184.
- [11] M. Vakili, M. Rafatullah, B. Salamatinia, A.Z. Abdullah, M.H. Ibrahim, K.B. Tan, P. Amouzgar, Application of chitosan and its derivatives as adsorbents for dye removal from water



- and wastewater: a review, *Carbohydr. Polym.*, 113 (2014) 115–130.
- [12] M. Malakootian, A. Fatehizadeh, Color removal from water by coagulation/caustic soda and lime, *Iran. J. Environ. Health. Sci. Eng.*, 7 (2010) 267–272.
- [13] M. Rafatullah, O. Sulaiman, R. Hashim, A. Ahmad, Adsorption of methylene blue on low-cost adsorbents: a review, *J. Hazard. Mater.*, 177 (2010) 70–80.
- [14] V. Katheresan, J. Kansedo, S.Y. Lau, Efficiency of various recent wastewater dye removal methods: a review, *J. Environ. Chem. Eng.*, 6 (2018) 4676–4697.
- [15] M.A.M. Salleh, D.K. Mahmoud, W.A.W.A. Karim, A. Idris, Cationic and anionic dye adsorption by agricultural solid wastes: a comprehensive review, *Desalination*, 280 (2011) 1–13.
- [16] Z.Y. Yang, Kinetics and mechanism of the adsorption of methylene blue onto ACFs, *J. China Univ. Mining Technol.*, 18 (2008) 437–440.
- [17] S. Karagöz, T. Tay, S. Ucar, M. Erdem, Activated carbons from waste biomass by sulfuric acid activation and their use on methylene blue adsorption, *Bioresour. Technol.*, 99 (2008) 6214–6222.
- [18] H.A. Al-Aoh, R. Yahya, M. Jamil Maah, M. Radzi Bin Abas, Adsorption of methylene blue on activated carbon fiber prepared from coconut husk: isotherm, kinetics and thermodynamics studies, *Desal. Water Treat.*, 52 (2014) 6720–6732.
- [19] A. Sharma, G. Sharma, M. Naushad, A.A. Ghfar, D. Pathania, Remediation of anionic dye from aqueous system using bio-adsorbent prepared by microwave activation, *Environ. Technol.*, 39 (2018) 917–930.
- [20] A. Sharma, G. Sharma, A. Kumar, Z.M. Siddiqi, D. Pathania, Exclusion of organic dye using neoteric activated carbon prepared from *Cornulaca monacantha* stem: equilibrium and thermodynamics studies, *Mater. Sci. Forum.*, 875 (2016) 1–15.
- [21] S. Rani, M. Aggarwal, M. Kumar, S. Sharma, D. Kumar, Removal of methylene blue and rhodamine B from water by zirconium oxide/graphene, *Water Sci.*, 30 (2016) 51–60.
- [22] H. Tavakkoli, F. Hamedi, Synthesis of  $Gd_{0.5}Sr_{0.5}FeO_3$  perovskite-type nanopowders for adsorptive removal of MB dye from water, *Res. Chem. Intermed.*, 42 (2016) 3005–3027.
- [23] L.Y. Chin, L.Y. Pei, R. Rosli, N.H. Mohd Atni, Immobilization of Nano-Sized  $TiO_2$  on Glass Plate for the Removal of Methyl Orange and Methylene Blue, M. Hashim, Ed., *ICGSCE 2014*, Springer, Singapore, 2015.
- [24] S.T. Yang, S. Chen, Y. Chang, A. Cao, Y. Liu, H. Wang, Removal of methylene blue from aqueous solution by graphene oxide, *J. Colloid Interface Sci.*, 359 (2011) 24–29.
- [25] G. Mustafa, H. Tahir, M. Sultan, N. Akhtar, Synthesis and characterization of cupric oxide (CuO) nanoparticles and their application for the removal of dyes, *Afr. J. Biotechnol.*, 12 (2013) 6650–6660.
- [26] H.A. Al-Aoh, I.A. Mihaina, M.A. Alsharif, A.A.A. Darwish, M. Rashad, S.K. Mustafa, H.S. Al-Shehri, Removal of methylene blue from synthetic wastewater by the selected metallic oxides nanoparticles adsorbent: equilibrium, kinetic and thermodynamic studies, *Chem. Eng. Commun.*, 207 (2019) 1719–1735.
- [27] D. Li, J. Yan, Z. Liu, Adsorption kinetic studies for removal of methylene blue using activated carbon prepared from sugar beet pulp, *Int. J. Environ. Sci. Technol.*, 13 (2016) 1815–1822.
- [28] M.T. Uddin, M.A. Rahman, M. Rukanuzzaman, M.A. Islam, A potential low-cost adsorbent for the removal of cationic dyes from aqueous solutions, *Appl. Water Sci.*, 7 (2017) 2831–2842.
- [29] J.J. Gao, Y.B. Qin, T. Zhou, D.D. Cao, P. Xu, D. Hochstetter, Y.F. Wang, Adsorption of methylene blue onto activated carbon produced from tea (*Camellia sinensis* L.) seed shells: kinetics, equilibrium, and thermodynamics studies, *J. Zhejiang Univ. Sci. B*, 14 (2013) 650–658.
- [30] A.A. Spagnoli, D.A. Giannakoudakis, S. Bashkova, Adsorption of methylene blue on cashew nutshell based carbons activated with zinc chloride: the role of surface and structural parameters, *J. Mol. Liq.*, 229 (2017) 465–471.
- [31] T. Yan, L. Wang, Adsorptive removal of methylene blue from aqueous solution by spent mushroom substrate: equilibrium, kinetics, and thermodynamics, *Bioresour. Technol.*, 8 (2013) 4722–4734.
- [32] M. Fatiha, B. Belkacem, Adsorption of methylene blue from aqueous solutions using natural clay, *J. Mater. Environ. Sci.*, 7 (2016) 285–292.
- [33] Y. Miyah, A. Lahrachi, M. Idrissi, Removal of cationic dye–methylene blue–from aqueous solution by adsorption onto corn cob powder calcined, *J. Mater. Environ. Sci.*, 7 (2016) 96–104.
- [34] H.A. Al-Aoh, Equilibrium, thermodynamic, and kinetic study for potassium permanganate adsorption by Neem leaves powder, *Desal. Water Treat.*, 170 (2019) 101–110.
- [35] R. Tang, C. Dai, C. Li, W. Liu, S. Gao, C. Wang, Removal of methylene blue from aqueous solution using agricultural residue walnut shell: equilibrium, kinetic, and thermodynamic studies, *J. Chem.*, 2017 (2017) 1–10.
- [36] I. Kaya, N. Yigit, M. Benli, Antimicrobial activity of various extracts of *Ocimum basilicum* L. and observation of the inhibition effect on bacterial cells by use of scanning electron microscopy, *Afr. J. Tradit. Complement. Altern. Med.*, 5 (2008) 363–369.
- [37] J.S. Melo, S.F. D'souza, Removal of chromium by mucilaginous seeds of *Ocimum basilicum*, *Bioresour. Technol.*, 92 (2004) 151–155.
- [38] D. Chakraborty, S. Maji, A. Bandyopadhyay, S. Basu, Biosorption of cesium-137 and strontium-90 by mucilaginous seeds of *Ocimum basilicum*, *Bioresour. Technol.*, 98 (2007) 2949–2952.
- [39] A. Gupte, M. Karjekar, J. Nair, Biosorption of copper using mucilaginous seeds of *Ocimum basilicum*, *Acta Biol. Indica*, 1 (2012) 113–119.
- [40] S. Shamsnejati, N. Chaibakhsh, A.R. Pendashteh, S. Hayeripour, Mucilaginous seed of *Ocimum basilicum* as a natural coagulant for textile wastewater treatment, *Ind. Crops Prod.*, 69 (2015) 40–47.
- [41] S.K. Theydan, M.J. Ahmed, Adsorption of methylene blue onto biomass-based activated carbon by  $FeCl_3$  activation: equilibrium, kinetics, and thermodynamic studies, *J. Anal. Appl. Pyrolysis*, 97 (2012) 116–122.
- [42] B.A. Fil, C. Ozmetin, M. Korkmaz, Cationic dye (methylene blue) removal from aqueous solution by montmorillonite, *Bull. Korean Chem. Soc.*, 33 (2012) 3184–3190.
- [43] D. Pathania, S. Sharma, P. Singh, Removal of methylene blue by adsorption onto activated carbon developed from *Ficus carica* bast, *Arabian J. Chem.*, 10 (2017) 1445–1451.
- [44] A. Guediri, A. Bouguettoucha, D. Chebli, N. Chafai, A. Amrane, Molecular dynamic simulation and DFT computational studies on the adsorption performances of methylene blue in aqueous solutions by orange peel-modified phosphoric acid, *J. Mol. Struct.*, 1202 (2020), doi: 10.1016/j.molstruc.2019.127290.
- [45] S.A. Odoemelam, U.N. Emeh, N.O. Eddy, Experimental and computational chemistry studies on the removal of methylene blue and malachite green dyes from aqueous solution by neem (*Azadirachta indica*) leaves, *J. Taibah Univ. Sci.*, 12 (2018) 255–265.
- [46] S. Patil, S. Renukdas, N. Patel, Removal of methylene blue, a basic dye from aqueous solutions by adsorption using teak tree (*Tectona grandis*) bark powder, *Int. J. Environ. Sci.*, 1 (2011) 711–726.
- [47] S.T. Ong, P.S. Keng, S.L. Lee, M.H. Leong, Y.T. Hung, Equilibrium studies for the removal of basic dye by sunflower seed husk (*Helianthus annuus*), *Int. J. Phys. Sci.*, 5 (2010) 1270–1276.
- [48] F. Ferrero, Dye removal by low cost adsorbents: hazelnut shells in comparison with wood sawdust, *J. Hazard. Mater.*, 142 (2007) 144–152.